# Spatially resolved stereoscopic surface profiling by using a feature-selective segmentation and merging technique

To cite this article: ChaBum Lee and Xiangyu Guo 2022 *Surf. Topogr.: Metrol. Prop.* **10** 014002

Surface Topography: Metrology and Properties

PAPER

# Spatially resolved stereoscopic surface profiling by using a feature-selective segmentation and merging technique

ChaBum Lee and Xiangyu Guo

J. Mike Walker '66 Department of Mechanical Engineering, Texas A&M University, 3123 TAMU, College Station, TX 77843-3123, United States of America

E-mail: cblee@tamu.edu

RECEIVED
27 December 2021

REVISED
21 February 2022

ACCEPTED FOR PUBLICATION
1 March 2022

PUBLISHED
15 March 2022

Keywords: 3D imaging, stereoscopy, surface profiling, feature segmentation, spatial resolution

## Abstract

We present a feature-selective segmentation and merging technique to achieve spatially resolved surface profiles of the parts by 3D stereoscopy and strobo-stereoscopy. A pair of vision cameras capture images of the parts at different angles, and 3D stereoscopic images can be reconstructed. Conventional filtering processes of the 3D images involve data loss and lower the spatial resolution of the image. In this study, the 3D reconstructed image was spatially resolved by automatically recognizing and segmenting the features on the raw images, locally and adaptively applying super-resolution algorithm to the segmented images based on the classified features, and then merging those filtered segments. Here, the features are transformed into masks that selectively separate the features and background images for segmentation. The experimental results were compared with those of conventional filtering methods by using Gaussian filters and bandpass filters in terms of spatial frequency and profile accuracy. As a result, the selective feature segmentation technique was capable of spatially resolved 3D stereoscopic imaging while preserving imaging features.

## Introduction

3D imaging process is to create the depth map in an image by manipulating 2D image data into 3D image data. In many industrial applications, 3D imaging techniques aid to identify the structures and patterns. Since 1832, when English physicist Sir Charles Wheatstone invented stereoscopy, several investigations on 3D imaging techniques such as interferometry, stereoscopy, time of flight (TOF), and structured light scanning have been performed [1]. While interferometry is typically used to scan smooth surfaces at a fraction of a wavelength [2], other techniques, such as single or dual cameras, are also available to provide millimeter-micrometer-resolution surface geometry [3]. Sheppard invented confocal scanning optical microscopy [4]. Guo estimated the geometry of rotating parts using stereoscopy and stroboscopy [5]. Kassamakov demonstrated a three-dimensional imaging approach based on Mirau interferometry for scanning grooved surfaces [6]. To generate super-resolution stereoscopic images, Song devised an approach for assuring stereo consistency across stereo image pairings [7]. Yan demonstrated how to adjust the disparity range of stereoscopic image pairings, so resolving the disocclusion problem [8]. Compared to interferometry and microscopy, the stereoscopy technique is widely utilized in the industry because of its simple structure composition and resistance to environmental influences.

The industry desires high-precision and accurate image reconstruction and fully automated part measurement and inspection. Denoising, contract enhancement techniques, and machine learning algorithms that produce high-quality images while maintaining imaging features are critical for image standardization and generalization in a wide variety of industrial applications [6, 9, 10]. For inspecting measurement samples, 3D machine vision-based imaging techniques for 3D surface profiling, reconstruction, and feature definition have been widely reported published. By increasing the picture sampling and spatial resolution of high-frequency signals via computer vision techniques, super-resolution imaging approaches based on deep learning algorithms improve image quality [6, 11, 12]. These techniques produce more lifelike and can be used for a variety of high-resolution microscopy applications. However, because of

the complexity of the technique, creating super-resolution photos from a collection of low-resolution images demands considerable computational effort and expense [13].

Along with advancements in 3D imaging technologies and image synthesis, numerous research has shown the potential for machine learning or artificial intelligence algorithms to improve image quality significantly. The super-resolution imaging technology overcomes the spatial limits of optical imaging systems by mixing low-resolution noisy blurring images with the high-resolution image. By adaptively estimating the point spread function, Yoo built an ideal super-resolution image network [14]. Dong trained a deep learning algorithm to map low- and high-resolution images [15]. To achieve high spatial resolution images, multiple machine learning or artificial intelligence-based technologies were applied. Because super-resolution imaging techniques are computationally prohibitively expensive for large-scale imaging [16, 17], they have been mainly used to imaging a small area or volume, with a particular focus on microscopy [18].

The 3D vision system must be fast, robust, small, and economical to get target measurements in macro-scale for online measurement. In this article, raw 3D images of a few tens of millimeter-sized samples were segmented based on their features adaptively. Rather than enhancing the full image at once, the quality of each segmented image was improved by using a super-resolution method to minimize computational complexity. As a result, the segmented images were reconstructed. This proposed technique for selective feature segmentation and merging combines automated feature classification, feature-based adaptive image segmentation, and image reconstruction can achieve high accuracy, precision, and spatial resolution in 3D surface profiling while retaining imaging features.

While the 3D recognition is commonly applied on the medical imaging processing [19, 20] and remote sensing field [21, 22], the proposed technique is aimed at online manufacturing inspection. Based on the 3D reconstruction from the stereoscopy system, the implemented selective feature segmentation and merging can effectively recognize the desired structures or patterns. This technique can be applied for the roll-to-roll, molded inspection. Further with the development of micro-stereoscopic technique, and random feature classification, it can be applied for surface defects inspection on freeform based structure.

## Imaging method

The feature-selective segmentation (FSS) is basically based on the feature separation technique to apply the filters for 3D image quality enhancement adaptively. Filtering technology is a natural way to extract surface information, as well as multi-scalar features of 3D surface [23]. Low frequency presents spaced irregularity on the sampled surfaces, or the profile information surface profile, while the high frequency presents the roughness and irrelevant form noise caused by the environment. Thus, a low-pass filter can be applied to generate the fitted surface map and a high-pass filter is capable of removing the roughness or the environmental noise information.

The definition to low-pass filter is defined below, where $H(u, v)$ is a filter function, $\omega_0$ is a cutoff frequency, (u,v) is a point on the frequency domain. The high-pass filter is defined in the opposite way. The filtering process can be implemented via Fourier transform.

$$H(u, v) = \begin{cases} 1 \; if \sqrt{u^2 + v^2} \leqslant \omega_0 \\ 0, \; otherwise \end{cases} \tag{1}$$

In this study, stereoscopy was employed for 3D imaging, and the FSS method was tested on the stereoscopic system. The Stereo Camera Calibrator app in MATLAB was used for the calibration [5]. Twenty images of the calibration checkerboard pattern at different orientations regarding the cameras were captured by the stereoscope system. The detailed checkerboard imaging process was explained in section 3.1. Figure 1 describes the FSS and merging method, which was achieved by the following steps: (1) lens aberration was removed to eliminate the image distortion, (2) 3D reconstructed surface map is made by the stereoscopic technique with the aberration-removed image pair, (3) the image was separated based on the features so that the background image and target image could be independently processed, (4) low-pass filter was applied first for the background and target image surface fitting. (5) two featured images were merged back to get the 3D image, and high-pass filter was applied for the noise deduction, (6) the 3D image and profile were achieved by linear extraction.

The FSS method was validated with a simple structure (ø10 mm and thickness 2 mm), and showed good spatial resolution. The features are transformed into masks that selectively separate the features and background images for segmentation. Two different features were used to validate and evaluate the FSS performance. The final image and the A-A' profile shown in figure 1 showed that the 3D image was successfully obtained. As a result, the FSS and merging method improved the 3D reconstructed image that is spatially resolved while preserving imaging features.

## Experiments

### Stereoscopy based on feature-selective segmentation and merging method

The stereoscopic technique is embedded with a pair of vision cameras capturing images of the measurement target. By applying the triangulation, lens equation, and aberration elimination method, the 3D image, the so-called depth map, is reconstructed by the location

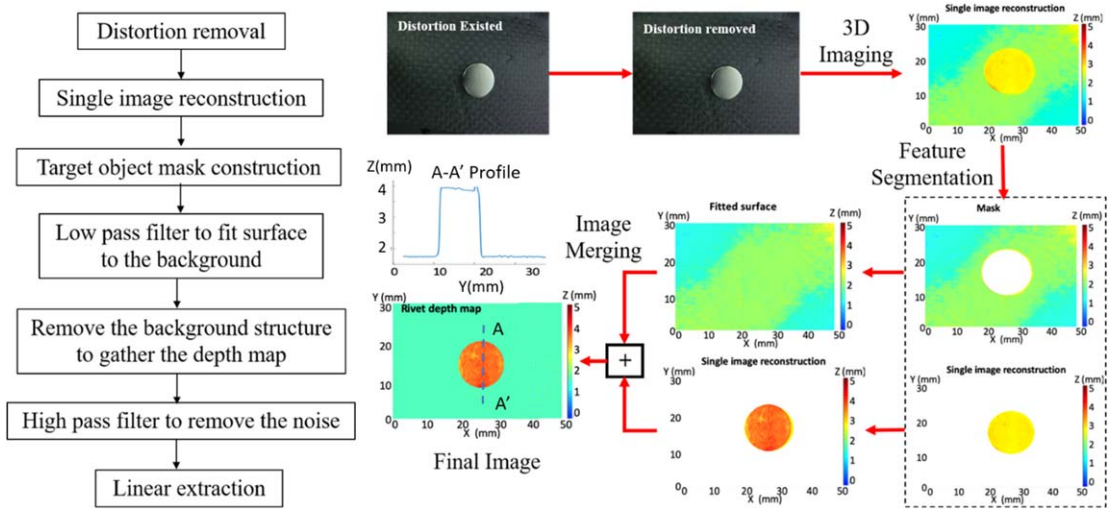


**Figure 1.** Feature-selective segmentation and merging: flow chart (left) and preliminary experiment results (right).

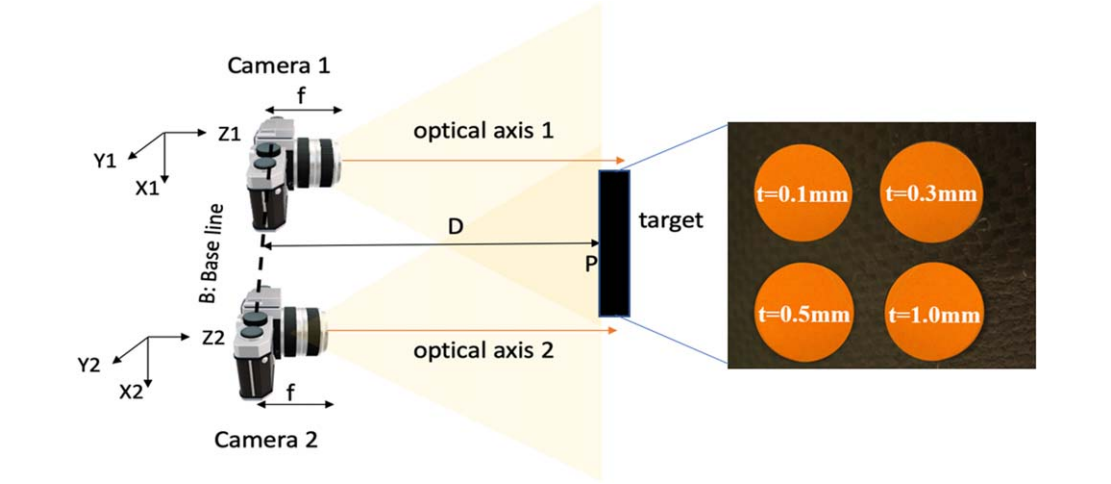


**Figure 2.** Experimental setup for stereoscopic 3D imaging.

information of the same object points from both the left and right images. Figure 2 shows the principle of the stereoscopic imaging process. Camera 1 and 2 have their coordinate system on the charge-coupled device (CCD) frame. Here, f is the focal length of the lens, and B is the distance between two cameras. The image depth information D from the point P on the target to the CCD of the camera system can be calculated by [11],

$$D = f\left(\frac{B}{y_2 - y_1} - 1\right) \tag{2}$$

A stereo camera calibration is performed to determine the intrinsic and extrinsic camera parameters or the projection matrix coefficients of the system [24]. These parameters transfer the scene points in 3D space to their corresponding image points, thus the measured depth can be recovered. In this study, calibration was performed with the same camera systems for the target sample measurement. The measurement target was fabricated by attaching metal stickers with different thickness (t) with 0.1, 0.3, 0.5, 1.0 mm and the diameter (ø10 mm) on the flat plate. As two cameras size are 29 by 29 mm (camera model: Basler aca5472-17 um and lens ML-U1217SR-18C), which allows the baseline B to be set as 50mm. The D is set to be 300 mm away from the target.

Figure 3 shows the 3D reconstructed results comparison. The single reconstructed image was obtained by the stereoscopic methods on the distortion-removal images. The information of each pattern is related to the base structure, thus FSS method was applied to remove such effect. By identify the circular pattern's radius and center location, mask can be generated to separate the background and target information. The fitted background was generated by the bandpass filter combined with the low-pass filter and the high-pass filter was applied after the merging process. Each of the pattern information was extracted

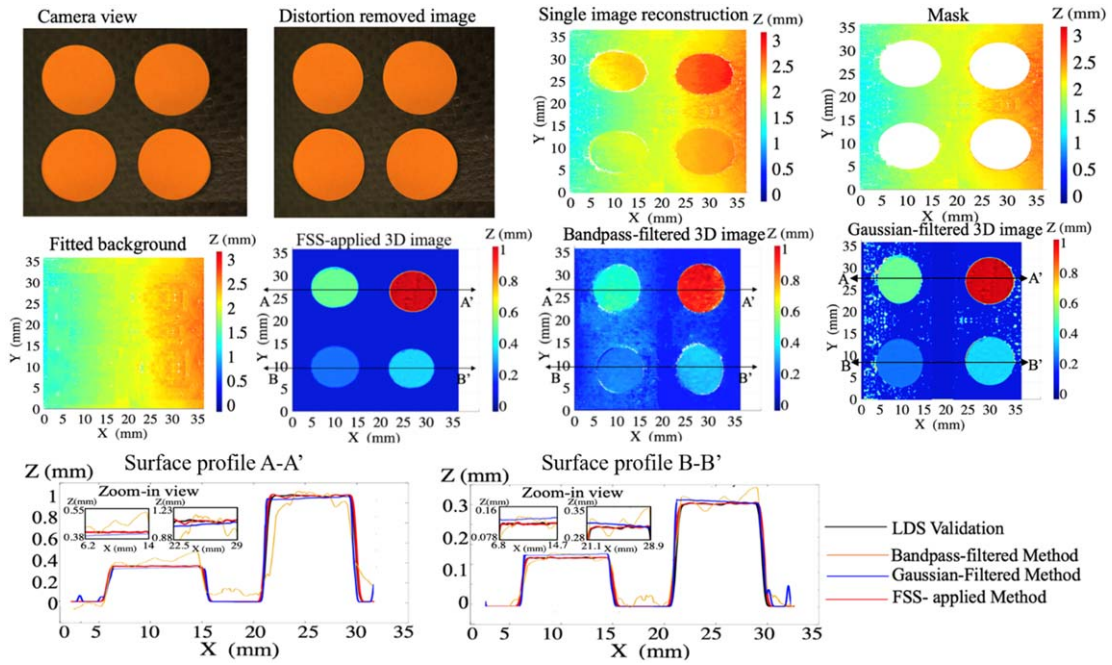


**Figure 3.** 3D imaging results: FSS, bandpass-filtered, gaussian-filtered 3D images.

from the base structure. The FSS result is compared with the general bandpass filtered method, the gaussian-filtered method and reference measurement by the laser displacement sensor with 20 nm resolution.

Instead of separating the target information from the background, the conventional filtering method is based on the polynomial method to find the best fitted plan to the stereoscopic reconstructed map, then extract the pattern features. This method can present the target location and rough depth information, but the cross-talk effect between the pattern and base structure exists. The pattern profiles by the bandpass-filtered 3D imaging also showed a significant discrepancy with those of the laser displacement sensor. The Gaussian filter to the base structure was applied here for the comparison as well. This method can extract the pattern information well but the edge-effect, which is the noise information from the edge of image frame, exists, and we can observe this from the reconstructed map and the linear scan. Same high-pass filter was applied to remove the environmental noise for both methods.

This result shows that the filtering process applied to all features, including the patterns and background, involves the data, and bandpass filtering of the images involves data loss and lowers the spatial resolution of the image. The surface profiles of the FSS-applied 3D imaging method showed good agreement with the laser displacement sensor output, and the discrepancy was estimated at less than 1%. This result indicates that the 3D reconstructed image was spatially resolved by automatically recognizing and segmenting the features on the 2D images, locally and adaptively applying super-resolution algorithm to the segmented images based on the classified features, and then merging those filtered segments. As a result, the FSS and merging method is confirmed to significantly enhance the spatial resolution of the 3D stereoscopic images while preserving imaging features.

## Strobo-stereoscopy based on feature-selective segmentation and merging method

Guo combined stroboscopy and stereoscopy, enabling in-process 3D imaging while the measurement target is rotating [5], and recently introduced fluorescence strobo-stereoscopy to suppress specular reflection off the optical quality rod and patterned roll [25]. In this study, the FSS and merging method and strobo-stereoscopy algorithm were combined to in-process obtain spatially resolved 3D images of the rotating target, as seen in figure 4. While the stereoscopy algorithm can provide a 3D image at a specific measurement position, the phase-shifting of the strobo-light allows the whole-view reconstruction of the rotating target while the target is rotating with a frequency. The quadrature encoder outputs are feedback for the stroboscopic light on/off control, so the specific area of the measurement target can be illuminated by blinking the light-emitting diode (LED) light. The 3D images were obtained at every 20-degree interval. The illumination system and camera system can be synchronized with the spindle motion. The 18 3D images reconstructed around the rod were systematically stitched to generate the full view image.

The stereoscopic image processing algorithm is typically for single image reconstruction. The phase unwrapping is required for the curve surface stitching process. In order to stitch the neighboring images

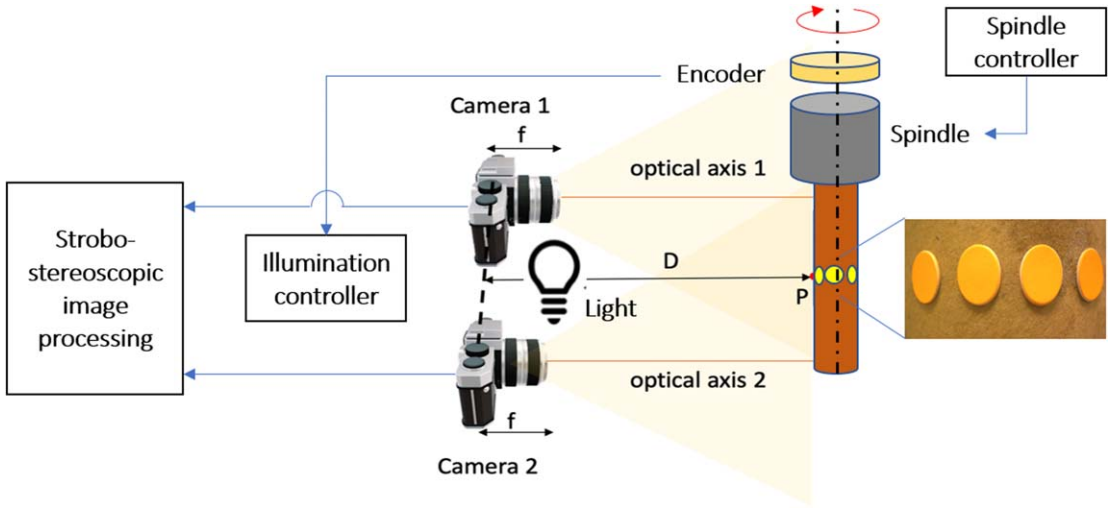


**Figure 4.** Experimental setup for strobo-stereoscopic 3D imaging.

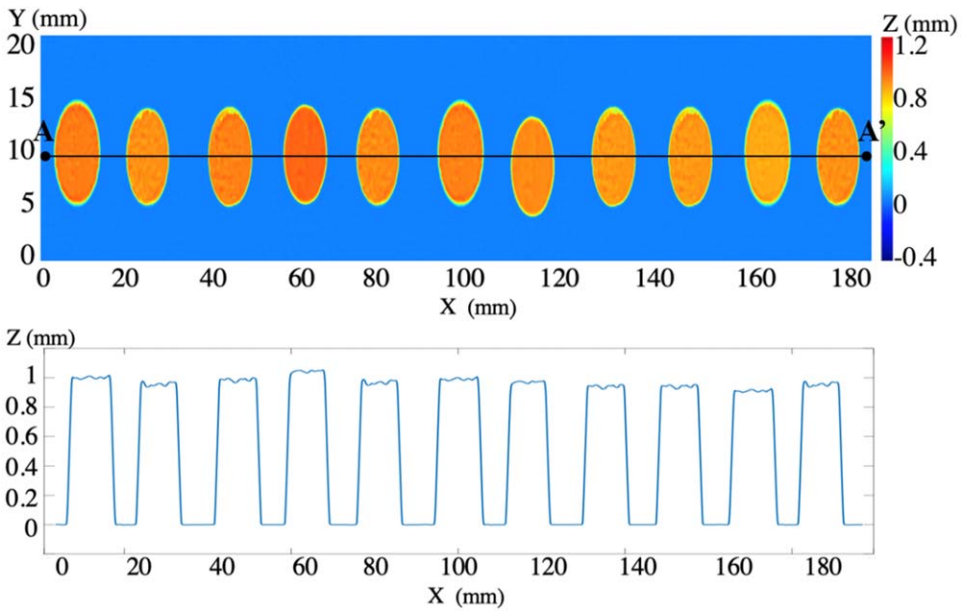


**Figure 5.** FSS-applied strobo-stereoscopic 3D image: full-view image (top) and A–A' profile (bottom).

conveniently and efficiently, FSS method were applied to the raw reconstructed surface map, thus the curve information from the base structure can be removed only the target information remained. The panorama full view map was reconstructed through the neighboring images stitching by defining the location of the overlapped patterns. Finally, 3D full-view stereoscopic images were obtained. The whole measurement and imaging processing operations were automated in the LABVIEW and MATLAB software environment, and the whole process took less than 1 s. In the experiment, the patterns were simply made by attaching the metal stickers (ø10 mm and 1 mm thickness). Those were randomly attached around the rod, and the rod was attached to the aerostatic spindle.

The FSS-applied strobo-stereoscopic 3D image was in-process obtained while the rod was rotating at a 100 revolution per minute (RPM). The reconstructed panorama full view image and the profile results showed that the pattern diameter, height, and interval were identified, as seen in figure 5. The isometric view and top view of the rod with the 1.0 mm thick patterns were successfully reconstructed as seen in figure 6.

In the same way, the metal stickers (ø10 mm and 0.1 mm thickness) were attached to the rod, and measured the 3D images as seen in figures 7 and 8. Those

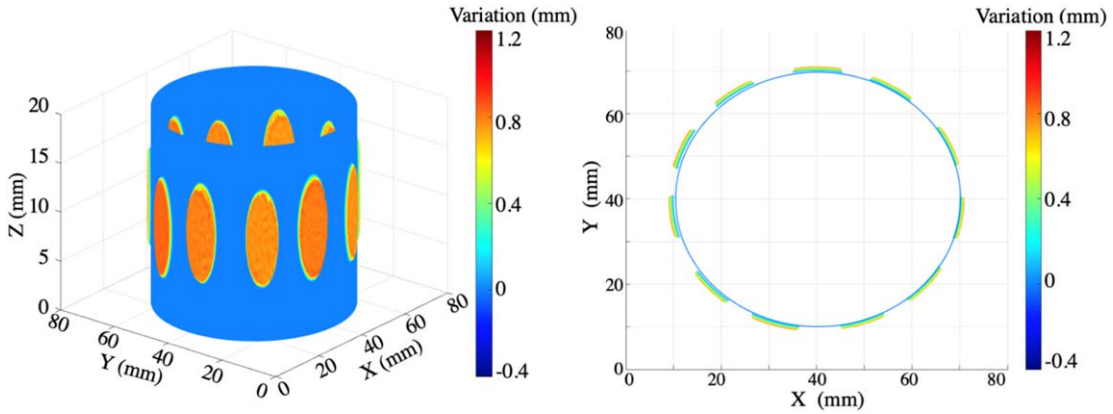


**Figure 6.** 3D strobo-stereoscopic image reconstruction results: isometric view (left) and top view (right).

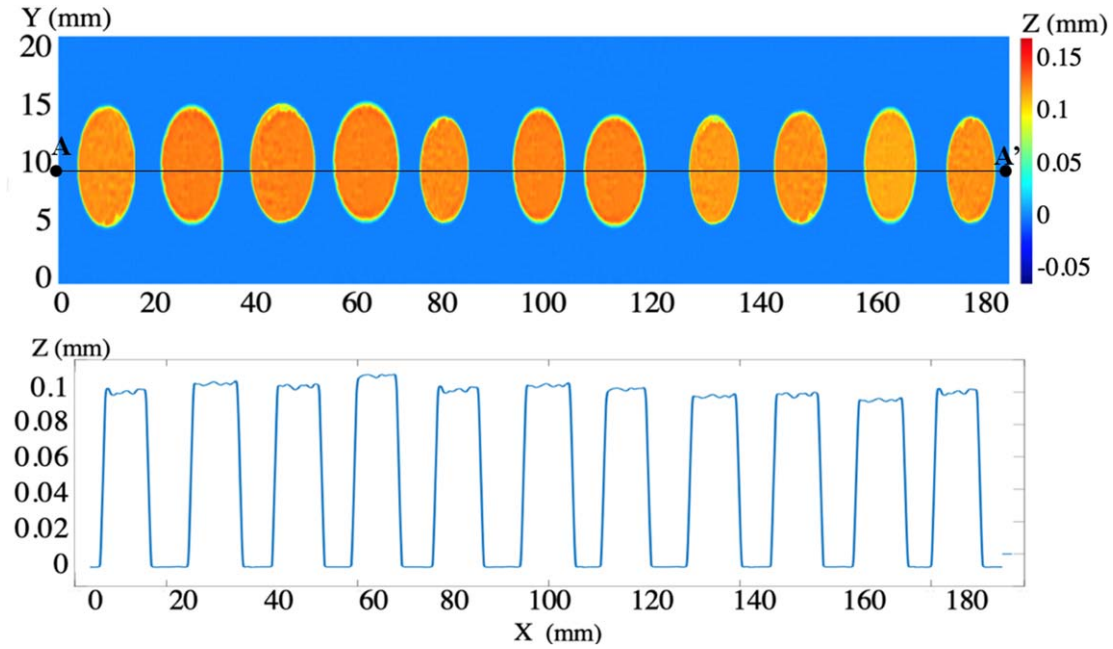


**Figure 7.** FSS-applied strobo-stereoscopic 3D image: full-view image (top) and A–A' profile (bottom).

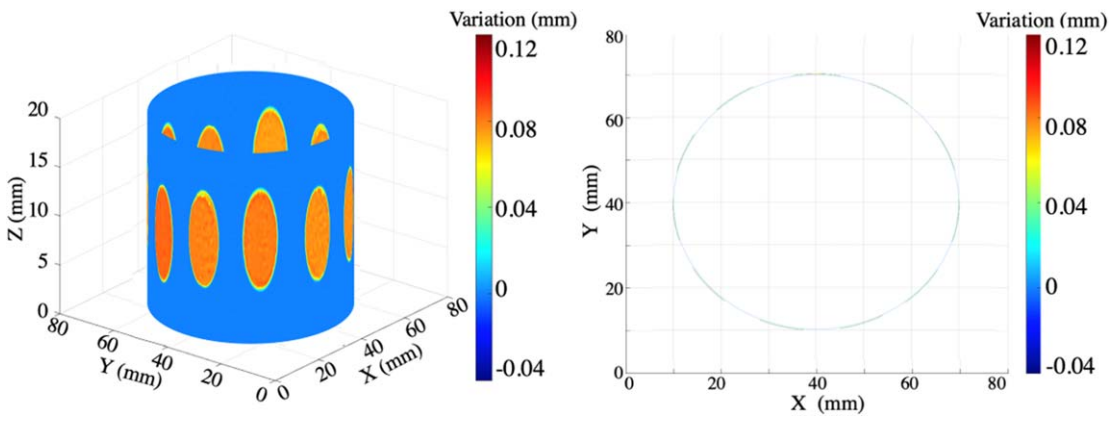


**Figure 8.** 3D strobo-stereoscopic image reconstruction results: isometric view (left) and top view (right).

results showed the potential of the FSS and merging method applicable to microscopy applications.

## Conclusion

The FSS and merging algorithm were implemented in the 3D imaging process for conventional stereoscopy and strobo-stereoscopy. The FSS image processing method was experimentally validated by reconstructing 3D stereoscopic images of the stationary and rotating targets. The image processing algorithm and convenient image stitching algorithm were developed to selectively separate the features from the background image and create a full-view image. The whole measurement and imaging processing were automated. The experimental results showed that the FSS-processed 3D imaging method provides spatially resolved images compared with the conventional image filtering processes. The proposed 3D imaging method has a high potential to be adapted in various industrial applications requiring 3D visions. The feature extraction algorithms for various pattern shapes will be developed for future work, and those analysis methods for surface metrology and inspection will be studied. Also, the high-speed camera systems will be included to extend the measurement capability available for high-speed 3D imaging.

## Acknowledgments

This research has been supported by Ministry of Trade, Industry and Energy (KEIT, Project No. 20011498, Robotic CFRP-metal mechanical joining and adhesive bonding process for future automotive applications).

## Data availability statement

The data that support the findings of this study are available upon reasonable request from the authors.

## Disclosures

Authors declare no conflicts of interest.

## ORCID iDs

ChaBum Lee https://orcid.org/0000-0002-0053-6863

## References

[1] Wheatstone S C 2021 *Oxford Dictionaries, Retrieved* **28**
[2] Hariharan P 2010 *Basics of Interferometry* (Boston: Academic)
[3] Zhang Y *et al* 2015 A fast 3D reconstruction system with a low-cost camera accessory *Sci. Rep.* **5** 10909
[4] Sheppard C J R and Hamilton D K 1983 High resolution stereoscopic imaging *Appl. Opt.* **22** 886–7
[5] Xiangyu G and Lee C B 2021 Preliminary study of phase-shifting strobo-stereoscopy for cutting tool monitoring *J. Manuf. Processes* **64** 1214–22
[6] Kassamakov I, Lecler S, Nolvi A, Nolvi A, Leong-Hoï A, Montgomery P and Hæggström E 2017 3D Super-resolution optical profiling using microsphere enhanced mirau interferometry *Scientific Report* **7** 3683
[7] Song W, Choi S-il, Jeong S and Sohn K *Stereoscopic Image Super-Resolution with Stereo Consistent Feature, The Thirty-Fourth AAAI Conf. on Artificial Intelligence, 2020.*
[8] Yan T, Jiao J, Liu W and Lau R W H 2019 Stereoscopic image generation from light field with disparity scaling and super-resolution *IEEE Trans. Image Process.* **29** 1827–42
[9] Eun D-in, Jang R, Ha W S, Lee H, Jung S C and Kim N 2020 Deep-learning-based imaging quality enhancement of compressed sensing magnetic resonance imaging of vessel wall: comparison of self-supervised and unsupervised approaches *Sci. Rep.* **10** 13950
[10] Khan R, Yang Y, Liu Q, Shen J and Li B 2021 Deep imaging enhancement for ill light imaging *J. Opt. Soc. Am. A* **38** 827–39
[11] Yoo S B and Lee E-J 2021 *Deep Super-Resolution Imaging Technology: Toward Optical Super-Vision, in IEEE Consumer Electronics Magazine* **10** 24–31
[12] Sahin E, Katkovnik V and Gotchev A 2016 Super-resolution in a defocused plenoptic camera: A wave-optics-based approach *Opt. Lett.* **41** 998–1001
[13] Zeng Z-ping, Xie H, Chen L, Zhangha K, Zhao K, Yang X-san and Xi P 2017 Computational methods in super-resolution microscopy *Frontiers Inf Technol Electronic Eng* **18** 1222–35
[14] Yoo S B and Lee E-J 2020 Deep super-resolution imaging technology: toward optical super-vision *IEEE Consumer Electronics Magazine* **10** 24–31
[15] Dong C, Loy C C, He K and Tang X 2014 Learning a deep convolutional network for image super-resolution *European Conference on Computer Vision* **2014** 184–99
[16] Farsiu S, Robinson D, Elad M and Milanfar P 2004 *Advances and challenges in super-resolution, International Journal of Imaging Systems Technology* **14** 47–57
[17] Ellis M A and Walker W F Super-resolution image reconstruction with reduced computational complexity *2009 IEEE Int. Ultrasonic Symp. (20-23 September) (Rome, Italy)*
[18] Schubert V 2017 Super-resolution microscopy—applications in plant cell research *Front. Plant Sci.* **8** 531
[19] Suri J S, Singh S and Reden L 2002 Computer vision and pattern recognition techniques for 2D and 3D MR cerebral cortical segmentation (Part I): a state-of-the-art review *Pattern Analysis & Applications* **5** 46–76
[20] Remeseiro B and Veronica B-C 2019 A review of feature selection methods in medical applications *Comput. Biol. Med.* **112** 103375
[21] Shao F, Li K, Lin W, Jiang G and Yu M 2015 Using binocular feature combination for blind quality assessment of stereoscopic images *IEEE Signal Process Lett.* **22** 1548–51
[22] Simonetto E, Oriot H and Garello R 2005 Rectangular building extraction from stereoscopic airborne radar images *IEEE Trans. Geosci. Remote Sens.* **43** 2386–95
[23] Stout K J and Blunt L (ed) 2000 *Part III - Filtering Technology for Three-Dimensional Surface Topography Analysis: Three Dimensional Surface Topography* (Butterworth-Heinemann) 95–142
[24] Faugeras O 1993 *Three-Dimensional Computer Vision: a Geometric Viewpoint* (MIT press)
[25] Xiangyu G and Lee C B 2022 Fluorescence strobo-stereoscopy for specular reflection-suppressed full field of view imaging *Measurement* **192** 11090